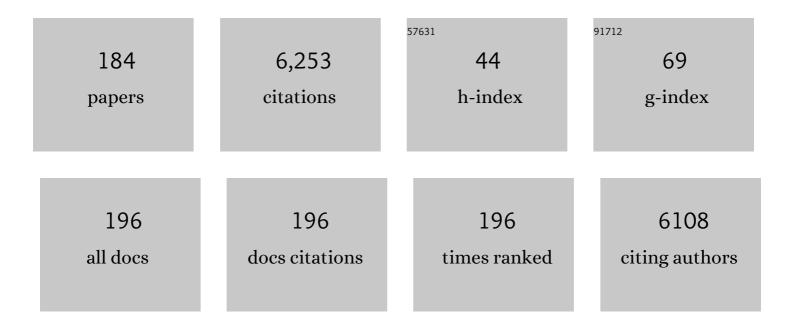
List of Publications by Year in descending order

Source: https://exaly.com/author-pdf/4860415/publications.pdf Version: 2024-02-01



#	Article	IF	CITATIONS
1	Three human RNA polymerases interact with TFIIH via a common RPB6 subunit. Nucleic Acids Research, 2022, 50, 1-16.	6.5	13
2	Characteristic H3 N-tail dynamics in the nucleosome core particle, nucleosome, and chromatosome. IScience, 2022, 25, 103937.	1.9	5
3	Histone tail network and modulation in a nucleosome. Current Opinion in Structural Biology, 2022, 75, 102436.	2.6	8
4	Structural and dynamical insights into the PH domain of p62 in human TFIIH. Nucleic Acids Research, 2021, 49, 2916-2930.	6.5	10
5	Difference of binding modes among three ligands to a receptor mSin3B corresponding to their inhibitory activities. Scientific Reports, 2021, 11, 6178.	1.6	10
6	Density-Functional Tight-Binding Parameters for Bulk Zirconium: A Case Study for Repulsive Potentials. Journal of Physical Chemistry A, 2021, 125, 2184-2196.	1.1	2
7	Is Oxygen Diffusion Faster in Bulk CeO2 or on a (111)-CeO2 Surface? A Theoretical Study. Chemistry Letters, 2021, 50, 568-571.	0.7	4
8	Quantum Chemical Calculations for up to One Hundred Million Atoms Using D <scp>cdftbmd</scp> Code on Supercomputer Fugaku. Chemistry Letters, 2021, 50, 1546-1550.	0.7	7
9	The N-terminal Tails of Histones H2A and H2B Adopt Two Distinct Conformations in the Nucleosome with Contact and Reduced Contact to DNA. Journal of Molecular Biology, 2021, 433, 167110.	2.0	16
10	Quantum-Mechanical Molecular Dynamics Simulations on Secondary Proton Transfer in Bacteriorhodopsin Using Realistic Models. Journal of Physical Chemistry B, 2021, 125, 10947-10963.	1.2	10
11	Mechanism of hERG inhibition by gating-modifier toxin, APETx1, deduced by functional characterization. BMC Molecular and Cell Biology, 2021, 22, 3.	1.0	5
12	Recent advances in quantumâ€mechanical molecular dynamics simulations of proton transfer mechanism in various waterâ€based environments. Wiley Interdisciplinary Reviews: Computational Molecular Science, 2020, 10, e1419.	6.2	10
13	Partial Replacement of Nucleosomal DNA with Human FACT Induces Dynamic Exposure and Acetylation of Histone H3 N-Terminal Tails. IScience, 2020, 23, 101641.	1.9	15
14	Acetylated histone H4 tail enhances histone H3 tail acetylation by altering their mutual dynamics in the nucleosome. Proceedings of the National Academy of Sciences of the United States of America, 2020, 117, 19661-19663.	3.3	31
15	Hydroxide Ion Carrier for Proton Pumps in Bacteriorhodopsin: Primary Proton Transfer. Journal of Physical Chemistry B, 2020, 124, 8524-8539.	1.2	16
16	Hierarchical parallelization of divideâ€andâ€conquer density functional tightâ€binding molecular dynamics and metadynamics simulations. Journal of Computational Chemistry, 2020, 41, 1759-1772.	1.5	10
17	Spinâ€flip approach within timeâ€dependent density functional tightâ€binding method: Theory and applications. Journal of Computational Chemistry, 2020, 41, 1538-1548.	1.5	12
18	Cover Image, Volume 10, Issue 1. Wiley Interdisciplinary Reviews: Computational Molecular Science, 2020, 10, e1459.	6.2	1

#	Article	IF	CITATIONS
19	Confined water-mediated high proton conduction in hydrophobic channel of a synthetic nanotube. Nature Communications, 2020, 11, 843.	5.8	116
20	Large-Scale Molecular Dynamics Simulation for Ground and Excited States Based on Divide-and-Conquer Long-Range Corrected Density-Functional Tight-Binding Method. Journal of Chemical Theory and Computation, 2020, 16, 2369-2378.	2.3	22
21	The Eaf3 chromodomain acts as a pH sensor for gene expression by altering its binding affinity for histone methylated-lysine residues. Bioscience Reports, 2020, 40, .	1.1	4
22	Structural visualization of key steps in nucleosome reorganization by human FACT. Scientific Reports, 2019, 9, 10183.	1.6	42
23	Sodium―and Potassiumâ€Hydrate Melts Containing Asymmetric Imide Anions for Highâ€Voltage Aqueous Batteries. Angewandte Chemie - International Edition, 2019, 58, 14202-14207.	7.2	81
24	Sodium―and Potassiumâ€Hydrate Melts Containing Asymmetric Imide Anions for Highâ€Voltage Aqueous Batteries. Angewandte Chemie, 2019, 131, 14340-14345.	1.6	18
25	GPUâ€Accelerated Largeâ€Scale Excitedâ€State Simulation Based on Divideâ€andâ€Conquer Timeâ€Dependent Densityâ€Functional Tightâ€Binding. Journal of Computational Chemistry, 2019, 40, 2778-2786.	1.5	24
26	Development of Large-Scale Excited-State Calculations Based on the Divide-and-Conquer Time-Dependent Density Functional Tight-Binding Method. Journal of Chemical Theory and Computation, 2019, 15, 1719-1727.	2.3	17
27	D <scp>cdftbmd</scp> : Divideâ€andâ€Conquer Density Functional Tightâ€Binding Program for Hugeâ€System Quantum Mechanical Molecular Dynamics Simulations. Journal of Computational Chemistry, 2019, 40, 1538-1549.	1.5	58
28	Development of Divideâ€andâ€Conquer Densityâ€Functional Tightâ€Binding Method for Theoretical Research on Liâ€Ion Battery. Chemical Record, 2019, 19, 746-757.	2.9	15
29	Surface Reaction Simulation based on Divide-and-Conquer Type Density Functional Tight-Binding Molecular Dynamics (DC-DFTB-MD) MethodÂ: Case for Proton Diffusion on Pt(111) Surface. Vacuum and Surface Science, 2019, 62, 486-491.	0.0	Ο
30	Divide-and-Conquer Density-Functional Tight-Binding Molecular Dynamics Study on the Formation of Carbamate lons during CO2 Chemical Absorption in Aqueous Amine Solution. Bulletin of the Chemical Society of Japan, 2018, 91, 318-318.	2.0	1
31	Parallel implementation of efficient charge–charge interaction evaluation scheme in periodic divideâ€andâ€conquer densityâ€functional tightâ€binding calculations. Journal of Computational Chemistry, 2018, 39, 105-116.	1.5	29
32	Rigorous p <i>K</i> <sub>a</sub> Estimation of Amine Species Using Density-Functional Tight-Binding-Based Metadynamics Simulations. Journal of Chemical Theory and Computation, 2018, 14, 351-356.	2.3	38
33	Density-Functional Tight-Binding Molecular Dynamics Simulations of Excess Proton Diffusion in Ice I <sub>h</sub> , Ice I <sub>c</sub> , Ice III, and Melted Ice VI Phases. Journal of Physical Chemistry A, 2018, 122, 33-40.	1.1	17
34	Release of DCDFTBMD Program. Journal of Computer Chemistry Japan, 2018, 17, A21-A27.	0.0	2
35	Sertraline, chlorprothixene, and chlorpromazine characteristically interact with the REST-binding site of the corepressor mSin3, showing medulloblastoma cell growth inhibitory activities. Scientific Reports, 2018, 8, 13763.	1.6	16
36	Structural Diversity of Nucleosomes Characterized by Native Mass Spectrometry. Analytical Chemistry, 2018, 90, 8217-8226.	3.2	15

#	Article	IF	CITATIONS
37	Structural Basis of Homology-Directed DNA Repair Mediated by RAD52. IScience, 2018, 3, 50-62.	1.9	49
38	NMR Screening of mSin3B Binding Compounds for the Interaction Inhibition with a Neural Repressor, NRSF/REST. , 2018, , 705-726.		0
39	Divide-and-Conquer-Type Density-Functional Tight-Binding Simulations of Hydroxide Ion Diffusion in Bulk Water. Journal of Physical Chemistry B, 2017, 121, 1362-1371.	1.2	38
40	Quantum Chemical Estimation of Acetone Physisorption on Graphene Using Combined Basis Set and Size Extrapolation Schemes. Journal of Physical Chemistry C, 2017, 121, 8999-9010.	1.5	5
41	Crystal structure of the overlapping dinucleosome composed of hexasome and octasome. Science, 2017, 356, 205-208.	6.0	77
42	Determination of the Solution Structure of Isolated Histone H2A-H2B Heterodimer by using CS-Rosetta. Biophysical Journal, 2017, 112, 488a.	0.2	0
43	Common TFIIH recruitment mechanism in global genome and transcription-coupled repair subpathways. Nucleic Acids Research, 2017, 45, 13043-13055.	6.5	83
44	Divide-and-Conquer Density-Functional Tight-Binding Molecular Dynamics Study on the Formation of Carbamate Ions during CO2 Chemical Absorption in Aqueous Amine Solution. Bulletin of the Chemical Society of Japan, 2017, 90, 1230-1235.	2.0	32
45	A mimetic of the mSin3-binding helix of NRSF/REST ameliorates abnormal pain behavior in chronic pain models. Bioorganic and Medicinal Chemistry Letters, 2017, 27, 4705-4709.	1.0	21
46	Development of density-functional tight-binding repulsive potentials for bulk zirconia using particle swarm optimization algorithm. AIP Conference Proceedings, 2017, , .	0.3	3
47	Impact of nucleic acid and methylated H3K9 binding activities of Suv39h1 on its heterochromatin assembly. ELife, 2017, 6, .	2.8	61
48	NMR Screening of mSin3B Binding Compounds for the Interaction Inhibition with a Neural Repressor, NRSF/REST. , 2017, , 1-22.		1
49	Three pillars for achieving quantum mechanical molecular dynamics simulations of huge systems: Divideâ€andâ€conquer, densityâ€functional tightâ€binding, and massively parallel computation. Journal of Computational Chemistry, 2016, 37, 1983-1992.	1.5	88
50	Dataset for the NMR structure of the intrinsically disordered acidic region of XPC bound to the PH domain of TFIIH p62. Data in Brief, 2016, 6, 571-577.	0.5	0
51	Long-term pulmonary complications of chemical weapons exposure in former poison gas factory workers. Inhalation Toxicology, 2016, 28, 343-348.	0.8	11
52	Solution structure of the isolated histone H2A-H2B heterodimer. Scientific Reports, 2016, 6, 24999.	1.6	28
53	Dynamics of the Extended String-Like Interaction ofÂTFIIE with the p62 Subunit of TFIIH. Biophysical Journal, 2016, 111, 950-962.	0.2	9
54	The Interaction Mode of the Acidic Region of the Cell Cycle Transcription Factor DP1 with TFIIH. Journal of Molecular Biology, 2016, 428, 4993-5006.	2.0	12

#	Article	IF	CITATIONS
55	Extended string-like binding of the phosphorylated HP1α N-terminal tail to the lysine 9-methylated histone H3 tail. Scientific Reports, 2016, 6, 22527.	1.6	23
56	Automatized Parameterization of DFTB Using Particle Swarm Optimization. Journal of Chemical Theory and Computation, 2016, 12, 53-64.	2.3	55
57	Automatized Parameterization of the Densityâ€functional Tightâ€binding Method. II. Twoâ€center Integrals. Journal of the Chinese Chemical Society, 2016, 63, 57-68.	0.8	13
58	Câ€ŧerminal acidic domain of histone chaperone human <scp>NAP</scp> 1 is an efficient binding assistant for histone H2Aâ€H2B, but not H3â€H4. Genes To Cells, 2016, 21, 252-263.	0.5	21
59	Contrasting mechanisms for CO2 absorption and regeneration processes in aqueous amine solutions: Insights from density-functional tight-binding molecular dynamics simulations. Chemical Physics Letters, 2016, 647, 127-131.	1.2	34
60	Divide-and-Conquer-Type Density-Functional Tight-Binding Molecular Dynamics Simulations of Proton Diffusion in a Bulk Water System. Journal of Physical Chemistry B, 2016, 120, 217-221.	1.2	53
61	Infrared absorption spectrum of the simplest deuterated Criegee intermediate CD2OO. Journal of Chemical Physics, 2016, 145, 044305.	1.2	6
62	Infrared identification of the Criegee intermediates syn- and anti-CH3CHOO, and their distinct conformation-dependent reactivity. Nature Communications, 2015, 6, 7012.	5.8	74
63	Mass Spectrometric Approach for Characterizing the Disordered Tail Regions of the Histone H2A/H2B Dimer. Analytical Chemistry, 2015, 87, 2220-2227.	3.2	10
64	Chargeâ€neutralization effect of the tail regions on the histone <scp>H</scp> 2 <scp>A</scp> / <scp>H</scp> 2 <scp>B</scp> dimer structure. Protein Science, 2015, 24, 1224-1231.	3.1	4
65	Nucleosome organization and chromatin dynamics in telomeres. Biomolecular Concepts, 2015, 6, 67-75.	1.0	10
66	Structural Insight into the Mechanism of TFIIH Recognition by the Acidic String of the Nucleotide Excision Repair Factor XPC. Structure, 2015, 23, 1827-1837.	1.6	30
67	Critical interpretation of CH– and OH– stretching regions for infrared spectra of methanol clusters (CH3OH) <i>n</i> ( <i>n</i> = 2–5) using self-consistent-charge density functional tight-binding molecular dynamics simulations. Journal of Chemical Physics, 2014, 141, 094303.	1.2	17
68	N-terminal phosphorylation of HP1α increases its nucleosome-binding specificity. Nucleic Acids Research, 2014, 42, 12498-12511.	6.5	63
69	Telomeric repeats act as nucleosome-disfavouring sequences in vivo. Nucleic Acids Research, 2014, 42, 1541-1552.	6.5	20
70	Mechanism of Back Electron Transfer in an Intermolecular Photoinduced Electron Transfer Reaction: Solvent as a Charge Mediator. ChemPhysChem, 2014, 15, 2945-2950.	1.0	16
71	Extended String Binding Mode of the Phosphorylated Transactivation Domain of Tumor Suppressor p53. Journal of the American Chemical Society, 2014, 136, 14143-14152.	6.6	45
72	Structural Characterization of the Histone Multimers in the Gas Phase using Ion Mobility Mass Spectrometry and Molecular Dynamics Simulation. Biophysical Journal, 2014, 106, 464a.	0.2	0

#	Article	IF	CITATIONS
73	Theoretical study of cellobiose hydrolysis to glucose in ionic liquids. Chemical Physics Letters, 2014, 603, 7-12.	1.2	26
74	Growth of carbon nanotubes via twisted graphene nanoribbons. Nature Communications, 2013, 4, 2548.	5.8	89
75	Stochastic Search of Molecular Cluster Interaction Energy Surfaces with Coupled Cluster Quality Prediction. The Phenylacetylene Dimer. Journal of Chemical Theory and Computation, 2013, 9, 3848-3854.	2.3	2
76	Gas-Phase Structure of the Histone Multimers Characterized by Ion Mobility Mass Spectrometry and Molecular Dynamics Simulation. Analytical Chemistry, 2013, 85, 4165-4171.	3.2	22
77	Conclusive Evidence of the Reconstituted Hexasome Proven by Native Mass Spectrometry. Biochemistry, 2013, 52, 5155-5157.	1.2	26
78	Function of homo- and hetero-oligomers of human nucleoplasmin/nucleophosmin family proteins NPM1, NPM2 and NPM3 during sperm chromatin remodeling. Nucleic Acids Research, 2012, 40, 4861-4878.	6.5	67
79	Intrinsic Nucleic Acid-Binding Activity of Chp1 Chromodomain Is Required for Heterochromatic Gene Silencing. Molecular Cell, 2012, 47, 228-241.	4.5	53
80	Dimerization-Initiated Preferential Formation of Coronene-Based Graphene Nanoribbons in Carbon Nanotubes. Journal of Physical Chemistry C, 2012, 116, 15141-15145.	1.5	87
81	Dramatic Reduction of IR Vibrational Cross Sections of Molecules Encapsulated in Carbon Nanotubes. Journal of the American Chemical Society, 2011, 133, 8191-8198.	6.6	36
82	A Free-Energy Landscape for Coupled Folding and Binding of an Intrinsically Disordered Protein in Explicit Solvent from Detailed All-Atom Computations. Journal of the American Chemical Society, 2011, 133, 10448-10458.	6.6	102
83	Structural and biochemical analyses of the human PAD4 variant encoded by a functional haplotype gene. Acta Crystallographica Section D: Biological Crystallography, 2011, 67, 112-118.	2.5	14
84	Deimination stabilizes histone H2A/H2B dimers as revealed by electrospray ionization mass spectrometry. Journal of Mass Spectrometry, 2010, 45, 900-908.	0.7	20
85	Temperature and pressure dependence of molecular adsorption on single wall carbon nanotubes and the existence of an "adsorption/desorption pressure gap― Carbon, 2010, 48, 1867-1875.	5.4	19
86	Side-Chain Conformational Changes of Transcription Factor PhoB upon DNA Binding: A Population-Shift Mechanism. Journal of the American Chemical Society, 2010, 132, 12653-12659.	6.6	14
87	Comparison between TRF2 and TRF1 of their telomeric DNA-bound structures and DNA-binding activities. Protein Science, 2009, 14, 119-130.	3.1	109
88	Analysis Of Side-chain Dynamics Of PhoB Dna Binding/transactivation Domain Using Molecular Dynamics Simulations. Biophysical Journal, 2009, 96, 299a.	0.2	0
89	Comparison of DNA-Binding Activities Between hTRF2 and hTRFl with hTRF2 Mutants. , 2008, , 743-751.		0
90	Thermal unfolding of proteins probed by laser spray mass spectrometry. Rapid Communications in Mass Spectrometry, 2008, 22, 1430-1436.	0.7	14

#	Article	IF	CITATIONS
91	Waterâ€mediated interactions between DNA and PhoB DNAâ€binding/transactivation domain: NMRâ€restrained molecular dynamics in explicit water environment. Proteins: Structure, Function and Bioinformatics, 2008, 71, 1970-1983.	1.5	31
92	Structural characterization of human general transcription factor TFIIF in solution. Protein Science, 2008, 17, 389-400.	3.1	6
93	Structural insight into the TFIIE–TFIIH interaction: TFIIE and p53 share the binding region on TFIIH. EMBO Journal, 2008, 27, 1161-1171.	3.5	51
94	Novel Structural and Functional Mode of a Knot Essential for RNA Binding Activity of the Esa1 Presumed Chromodomain. Journal of Molecular Biology, 2008, 378, 987-1001.	2.0	42
95	Interaction of Acetone with Single Wall Carbon Nanotubes at Cryogenic Temperatures: A Combined Temperature Programmed Desorption and Theoretical Study. Langmuir, 2008, 24, 7848-7856.	1.6	30
96	A Mass Spectrometric Approach to the Study of DNA-Binding Proteins:  Interaction of Human TRF2 with Telomeric DNA. Biochemistry, 2008, 47, 1797-1807.	1.2	39
97	Structural Polymorphism of Chromodomains in Chd1. Journal of Molecular Biology, 2007, 365, 1047-1062.	2.0	28
98	NMR Dynamics Distinguish Between Hard and Soft Hydrophobic Cores in the DNA-binding Domain of PhoB and Demonstrate Different Roles of the Cores in Binding to DNA. Journal of Molecular Biology, 2007, 367, 1093-1117.	2.0	10
99	I-motif and quadruplex-based device that can control a protein release or bind and release small molecule to influence biological processes. Bioorganic and Medicinal Chemistry, 2007, 15, 1275-1279.	1.4	25
100	Top-down analysis of basic proteins by microchip capillary electrophoresis mass spectrometry. Rapid Communications in Mass Spectrometry, 2006, 20, 1932-1938.	0.7	36
101	A protein recycling system for nuclear magnetic resonance-based screening of drug candidates. Analytical Biochemistry, 2006, 353, 99-107.	1.1	4
102	Evaluation of binding affinity of protein-mutant dna complexes in solution by laser spray mass spectrometry. Journal of the American Society for Mass Spectrometry, 2006, 17, 611-620.	1.2	16
103	Stability analysis for double-stranded DNA oligomers and their noncovalent complexes with drugs by laser spray. Journal of Mass Spectrometry, 2006, 41, 1086-1095.	0.7	18
104	Evaluation of protein-DNA binding affinity by electrospray ionization mass spectrometry. Journal of the American Society for Mass Spectrometry, 2005, 16, 116-125.	1.2	25
105	Investigation of molecular size of transcription factor TFIIE in solution. Proteins: Structure, Function and Bioinformatics, 2005, 61, 633-641.	1.5	11
106	Structural Insights into the Asymmetric Effects of Zinc-Ligand Cysteine Mutations in the Novel Zinc Ribbon Domain of Human TFIIEα for Transcription. Journal of Biochemistry, 2005, 138, 443-449.	0.9	3
107	The Neural Repressor NRSF/REST Binds the PAH1 Domain of the Sin3 Corepressor by Using its Distinct Short Hydrophobic Helix. Journal of Molecular Biology, 2005, 354, 903-915.	2.0	76
108	A Novel Zinc Finger Structure in the Large Subunit of Human General Transcription Factor TFIIE. Journal of Biological Chemistry, 2004, 279, 51395-51403.	1.6	32

#	Article	IF	CITATIONS
109	Selective dissociation of non-covalent bonds in biological molecules by laser spray. Journal of Mass Spectrometry, 2004, 39, 1053-1058.	0.7	24
110	Crystallization and preliminary X-ray diffraction studies on the DNA-binding domain of the transcriptional activator protein PhoB fromEscherichia coli. Acta Crystallographica Section D: Biological Crystallography, 2002, 58, 1862-1864.	2.5	0
111	NMR structure of the hrap1 myb motif reveals a canonical three-helix bundle lacking the positive surface charge typical of myb DNA-binding domains 1 1Edited by P. E. Wright. Journal of Molecular Biology, 2001, 312, 167-175.	2.0	55
112	Solution Structure of a Telomeric DNA Complex of Human TRF1. Structure, 2001, 9, 1237-1251.	1.6	77
113	Structural genomics projects in Japan. Progress in Biophysics and Molecular Biology, 2000, 73, 363-376.	1.4	49
114	Structural comparison of the PhoB and OmpR DNA-binding/transactivation domains and the arrangement of PhoB molecules on the phosphate box. Journal of Molecular Biology, 2000, 295, 1225-1236.	2.0	90
115	Solution structure of the transactivation domain of ATF-2 comprising a zinc finger-like subdomain and a flexiblesubdomain. Journal of Molecular Biology, 1999, 287, 593-607.	2.0	54
116	Two metal-binding sites in a lead ribozyme bound to competitively by Pb2+ and Mg2+ . Induced structural changes as revealed by NMR. FEBS Journal, 1998, 255, 727-733.	0.2	10
117	Solution structure of the DNA-binding domain of human telomeric protein, hTRF1. Structure, 1998, 6, 1057-1065.	1.6	56
118	Substitutions of Conserved Aromatic Amino Acid Residues in Subunit I Perturb the Metal Centers of theEscherichia coli bo-Type Ubiquinol Oxidaseâ€. Biochemistry, 1998, 37, 1632-1639.	1.2	19
119	Investigation of the Pyrimidine Preference by the c-Myb DNA-binding Domain at the Initial Base of the Consensus Sequence. Journal of Biological Chemistry, 1997, 272, 17966-17971.	1.6	20
120	A Protein Kinase Cδ-binding Protein SRBC Whose Expression Is Induced by Serum Starvation. Journal of Biological Chemistry, 1997, 272, 7381-7389.	1.6	77
121	Escherichia coli positive regulator OmpR has a large loop structure at the putative RNA polymerase interaction site. Nature Structural and Molecular Biology, 1997, 4, 28-31.	3.6	87
122	The cavity in the hydrophobic core of Myb DNA-binding domain is reserved for DNA recognition and trans-activation. Nature Structural Biology, 1996, 3, 178-187.	9.7	243
123	Determination of the NMR solution structure of a specific DNA complex of the Myb DNA-binding domain. Journal of Biomolecular NMR, 1995, 6, 294-305.	1.6	4
124	Comparison of the free and DNA-complexed forms of the DMA-binding domain from c-Myb. Nature Structural and Molecular Biology, 1995, 2, 309-320.	3.6	156
125	Scattering Phenomena and Their Applications to the Spectroscopy. III. Applications of Raman Scattering (II) Journal of the Spectroscopical Society of Japan, 1995, 44, 163-168.	0.0	0
126	A Raman Spectroscopic Study on Conformations of DNA Oligomers: A Dominant Effect of an AA:TT Sequence Over Those of AT:AT and TA:TA Sequences on Determining Conformations of DNA Duplexes. Nucleosides & Nucleotides, 1994, 13, 1467-1481.	0.5	2

#	Article	IF	CITATIONS
127	Solution structure of a specific DNA complex of the Myb DNA-binding domain with cooperative recognition helices. Cell, 1994, 79, 639-648.	13.5	486
128	Most compact hairpin-turn structure exerted by a short DNA fragment, d(GCGAAGC) in solution: an extraordinarily stable structure resistant to nucleases and heat. Nucleic Acids Research, 1994, 22, 576-582.	6.5	203
129	Crystallization and X-ray Studies of the DNA-binding Domain of OmpR Protein, a Positive Regulator Involved in Activation of Osmoregulatory Genes in Escherichia coli. Journal of Molecular Biology, 1994, 235, 780-782.	2.0	12
130	2-Methylimidazole Does Not Bind to (Octaethylporphinato)iron(III) Chloride in the Presence of Methanol: A Resonance Raman Study. Journal of the American Chemical Society, 1994, 116, 4107-4108.	6.6	6
131	Cytochromedaxial ligand of thebd-type terminal quinol oxidase fromEscherichia coli. FEBS Letters, 1993, 335, 13-17.	1.3	12
132	Structural Polymorphism of DNA and Its Recognizing-Proteins Seibutsu Butsuri, 1993, 33, 142-147.	0.0	0
133	Extraordinarily stable mini-hairpins: electrophoretical and thermal properties of the various sequence variants of d(GCFAAAGC)and their effect on DNA sequencing. Nucleic Acids Research, 1992, 20, 3891-3896.	6.5	140
134	Structure of a DNA octamer, d(CCTTAAGG)2 obtained by restrained molecular dynamics based on Raman and NMR data. Journal of Molecular Structure, 1991, 242, 119-133.	1.8	2
135	Laser Raman microscope: Application on biological samples Journal of the Spectroscopical Society of Japan, 1990, 39, 323-334.	0.0	0
136	Spectrophotometric and resonance Raman studies on the formation of phenolate and thiolate complexes of (octaethylporphinato)iron(III). Inorganic Chemistry, 1990, 29, 2803-2807.	1.9	22
137	Proton nuclear magnetic resonance studies of the structure of the Fc fragment of human immunoglobulin G1: Comparisons of native and recombinant proteins. Molecular Immunology, 1990, 27, 571-579.	1.0	43
138	Application of 13C Nuclear Magnetic Resonance Spectroscopy to Molecular Structural Analyses of Antibody Molecules1. Journal of Biochemistry, 1989, 105, 867-869.	0.9	34
139	Extraordinary stable structure of short single-stranded DNA fragments containing a specific base sequence: d(GCGAAAGC). Nucleic Acids Research, 1989, 17, 2223-2231.	6.5	86
140	Location of phosphorylation site and DNA-binding site of a positive regulator, OmpR, involved in activation of the osmoregulatory genes ofEscherichia coli. FEBS Letters, 1989, 249, 168-172.	1.3	50
141	Proton Nuclear Magnetic Resonance Study of a Selectively Deuterated Mouse Monoclonal Antibody: Use of Two-Dimensional Homonuclear Hartmann-Hahn Spectroscopy1. Journal of Biochemistry, 1989, 106, 361-364.	0.9	12
142	Epimerization and hydrolysis of etoposide analogues in aqueous solution Chemical and Pharmaceutical Bulletin, 1989, 37, 422-424.	0.6	15
143	Location of DNA-binding segment of a positive regulator, OmpR, involved in activation of theompFandompCgenes ofEscherichia coli. FEBS Letters, 1988, 242, 27-30.	1.3	45
144	Quantitative treatment of photochemical effects on ultraviolet resonance Raman spectroscopic intensities - application to enzymic cofactors containing dihydronicotinamide and their photochemically induced transients. Journal of the American Chemical Society, 1987, 109, 3514-3520.	6.6	17

#	Article	IF	CITATIONS
145	Ultraviolet resonance Raman bands of guanosine and adenosine residues useful for the determination of nucleic acid conformation. Journal of Raman Spectroscopy, 1987, 18, 221-227.	1.2	36
146	Local and overall conformations of DNA double helices with the A·T base pairs. Biochimica Et Biophysica Acta Gene Regulatory Mechanisms, 1986, 867, 256-267.	2.4	45
147	Anomalous temperature dependence of the phosphorus-31 nuclear magnetic resonance chemical shift in d(CCGG) and d(CCTAGG) at the junction of the pyrimidine stack followed by the purine stack Chemical and Pharmaceutical Bulletin, 1986, 34, 3987-3993.	0.6	3
148	Nuclear magnetic resonance study on the interaction of aclacinomycin-A with a deoxyribo-hexanucleotide pentaphosphate d(CCTAGG)2 in aqueous solution Chemical and Pharmaceutical Bulletin, 1986, 34, 4494-4499.	0.6	10
149	Raman and Solid State NMR Study on an Inclusion Compound of Aspartame with Cyclodextrin. Bulletin of the Chemical Society of Japan, 1986, 59, 93-96.	2.0	9
150	A Raman spectroscopic analysis of the sequence-dependent structures of oligo-DNA duplexes: d(CGCG)2, d(GCGC)2, d(GGCC)2, and d(CCGG)2 in aqueous solution. Spectrochimica Acta Part A: Molecular Spectroscopy, 1986, 42, 1101-1106.	0.1	5
151	Conformation-sensitive Raman lines of mononucleotides and their use in a structure analysis of polynucleotides: guanine and cytosine nucleotides. Journal of Molecular Structure, 1986, 146, 123-153.	1.8	104
152	Self-complementary tetradeoxyribonucleoside triphosphates convenient chemical preparation and spectroscopic studies in solution. Tetrahedron, 1986, 42, 501-513.	1.0	14
153	The structure of nucleosome core particles as revealed by difference Raman spectroscopy. Nucleic Acids Research, 1986, 14, 2583-2596.	6.5	17
154	In-Plane Vibrational Modes of Guanine from an abInitioMO Calculation. Bulletin of the Chemical Society of Japan, 1985, 58, 638-645.	2.0	42
155	Infrared spectrum of trans-acrolein. Chemical Physics, 1985, 100, 365-375.	0.9	44
156	In-plane vibrational modes of cytosine from an ab initio MO calculation. Chemical Physics, 1985, 98, 71-80.	0.9	46
157	Raman spectrum of a closed-circular DNA. Biopolymers, 1985, 24, 1107-1111.	1.2	7
158	An A-form poly(dG) · poly(dC) in H2O solution. Biopolymers, 1985, 24, 1841-1844.	1.2	47
159	Collective vibrational modes in molecular assembly of DNA and its application to biological systems. Low frequency Raman spectroscopy. Journal of Chemical Physics, 1985, 82, 531-535.	1.2	80
160	Increased stability of the higher order structure of chicken erythrocyte chromatin: nanosecond anisotropy studies of intercalated ethidium. Biochemistry, 1985, 24, 1291-1297.	1.2	21
161	Coupled dynamics between DNA double helix and hydrated water by low frequency Raman spectroscopy. Journal of Chemical Physics, 1985, 83, 5972-5975.	1.2	70
162	Structure-spectrum correlations in nucleic acids. I. Raman lines in the 600–700 cmâ^'1range of guanosine residue. Nucleic Acids Research, 1984, 12, 6901-6908.	6.5	52

#	Article	IF	CITATIONS
163	Time-resolved resonance Raman study of alkaline isomerization of ferricytochrome c. Biochemistry, 1984, 23, 6802-6808.	1.2	18
164	A Possible Correlation between DNA Conformation and the Mode of Action of Restriction Enzymes1. Journal of Biochemistry, 1984, 96, 1807-1811.	0.9	4
165	Internal motion of deoxyribonucleic acid in chromatin. Nanosecond fluorescence studies of intercalated ethidium. Biochemistry, 1983, 22, 6018-6026.	1.2	42
166	Dynamics of DNA in Chromatin and DNA Binding Mode to Core Protein. Journal of Biochemistry, 1983, 93, 665-668.	0.9	13
167	DIFFERENCE RAMAN SPECTROSCOPY WITH A STOPPED-FLOW DEVICE. , 1983, , 113-116.		Ο
168	Lifetime of Tyrosine Fluorescence in Nucleosome Core Particles1. Journal of Biochemistry, 1982, 91, 2047-2055.	0.9	22
169	Deuteration kinetics of N-methylacetamide by means of a stopped-flow multi-detector Raman spectrophotometry. Journal of Raman Spectroscopy, 1982, 12, 138-143.	1.2	4
170	In-plane vibrational modes in the uracil molecule from an ab initio MO calculation. Journal of the American Chemical Society, 1981, 103, 1354-1358.	6.6	106
171	Rate of photochemical protonation and electronic relaxation of excited 1, N6â€ethenoadenosine in its aqueous solution. Journal of Chemical Physics, 1981, 75, 3831-3837.	1.2	8
172	A Spectroscopic Study of Hydrogen-bonds Involving the 2-Thiouracil Residue. Bulletin of the Chemical Society of Japan, 1980, 53, 1881-1887.	2.0	11
173	On the base-stacking in the 5′-terminal cap structure of mRNA: a fluorescence study. Nucleic Acids Research, 1980, 8, 1107-1119.	6.5	33
174	On the Normal Modes of Vibration in the Uracil Residue—The Use of15N-Isotope Effects. Bulletin of the Chemical Society of Japan, 1979, 52, 1340-1345.	2.0	26
175	Raman spectra of flavins: avoidance of interference from fluorescence. Chemical Physics Letters, 1978, 59, 210-213.	1.2	41
176	Characterization of a few Raman lines of tryptophan. Journal of Raman Spectroscopy, 1978, 7, 282-287.	1.2	63
177	Crystallization of Arginine-, Formylmethionine-, Tyrosine-, and Glycine-Transfer RNAs from Escherichia coil. Journal of Biochemistry, 1978, 84, 369-375.	0.9	3
178	A vibronic coupling in a degenerate electronic state via a nuclear momentum and an antisymmetric Raman scattering tensor. Journal of Chemical Physics, 1977, 67, 1009.	1.2	11
179	RESONANCE RAMAN EFFECTS OF NUCLEOTIDES. Chemistry Letters, 1977, 6, 907-908.	0.7	5
180	The nature of the vibronic coupling in a metalloporphyrin and its Raman scattering. Journal of Molecular Spectroscopy, 1977, 68, 335-358.	0.4	13

#	Article	IF	CITATIONS
181	Raman spectra of transfer RNAs with ultraviolet lasers. Nature, 1976, 260, 173-174.	13.7	17
182	On the excited-state geometry of the adenine residue as revealed by a preresonance Raman effect. Journal of Raman Spectroscopy, 1974, 2, 609-621.	1.2	37
183	Spectral Difference of the A and B Forms of Deoxyribonucleic Acid. Bulletin of the Chemical Society of Japan, 1974, 47, 1043-1044.	2.0	15
184	Infrared Spectra of Deoxyribonucleic Acids with Different Base Compositions in Their D2O Solutions. Bulletin of the Chemical Society of Japan, 1973, 46, 3891-3892.	2.0	5